26

Intrinsic Nonlinearity in Geomaterials: Elastic Properties of Rocks at Low Strain

Donatella Pasqualini

EES-9, University of California, Los Alamos National Laboratory, Los Alamos, New Mexico 87545.
Correspondence: Donatella Pasqualini, Mail Stop D443, email: dondy@lanl.gov.

Abstract
The elastic properties of geomaterials are anomalous. Hysteresis with end point memory, slow dynamics, and linear variation of the resonance frequency with the strain are only some of these uncommon features. All these characteristics have been related to a nonclassical nonlinear elasticity. Chapter 1 introduces two strain regions where the experiments show different elastic behaviors. At low strain, rocks show their intrinsic nonlinearity until a strain material-dependent threshold, ϵ_{th}. A transition from linear to classical nonlinear behavior appears in this first region. For strains beyond ϵ_{th} the experimental data are contaminated by a complex nonequilibrium dynamics. Memory effects and conditioning complicate the characterization of the intrinsic nonlinearity of the sample and they do not allow a simple interpretation of the experimental data to prove the existence of anomalous nonclassical nonlinearity.

Keywords: Classical nonlinearity, conditioning, dynamical experiments, geomaterials, intrinsic nonlinearity, memory effects, nonequilibrium dynamics, nonlinearity

1. Introduction

Rocks are complex systems. Their extraordinary elastic properties are the manifestation of this complexity. The presence of hysteresis with end point memory (Cook and Hodgson, 1965, Gordon and Davis, 1967), long–time recovery relaxation phenomena (TenCate and Shankland, 1996, TenCate et al., 2000), and anomalous softening of the resonance frequency with strain (Johnson et al., 1996) are only some examples of the uncommon elastic properties of geomaterials. This experimental evidence led us to define rocks as anomalous nonlinear elastic materials. Several basic questions are still open about this nonlinearity.

In this chapter some recent experimental results are presented which help to better understand the nonlinearity of rocks. The focus of this chapter is to show the existence of a strain threshold, below which these materials show a classical nonlinear behavior, and beyond which complex memory and conditioning effects appear. These two regions are fundamental for understanding the nonlinear nature of rocks and to define the intrinsic nonlinear behavior of these materials. The key point is that beyond

this threshold the experimental data cannot be simply used to prove the existence of nonclassical behavior due to the presence of nonequilibrium dynamics.

2. Intrinsic Nonlinearity and Conditioning

Most of the measurements of nonlinear effects are performed by resonance bar experiments. A detailed description of this experiment is presented by TenCate et al. in this book. In this type of experiment the resonance frequency (f_R) dependence on the external force is analyzed as an indicator of nonlinearity: the system is linear if the resonance frequency peak does not change with the external force, whereas a change in f_R indicates nonlinearity. There are many materials in nature that exhibit elastic nonlinearity. For these materials the nonlinearity is shown as a quadratic softening of the f_R increasing the drive amplitude. This nonlinearity, known as *classical nonlinearity*, has been described by Landau and Lifshitz (1998) using a Taylor expansion of the bar's displacement in the strain. Instead of a quadratic softening, rocks show a linear softening with the drive amplitude that was interpreted as an indicator of an anomalous nonlinearity (Guyer and Johnson, 1999) as shown by Johnson in this book.

[AQ1]

In recent works (TenCate et al., 2004; Pasqualini et al., submitted) it was shown that this shift has to be interpreted carefully because the measurements can be contaminated by the presence of a nonequilibrium dynamics. The external force can bring the rock into a nonequilibrium state complicating the dynamical behavior and the interpretation of the nonclassical behavior. Figure 26.1 shows the effect of the conditioning on the resonance frequency peak. The peak of the resonance curve is measured at different

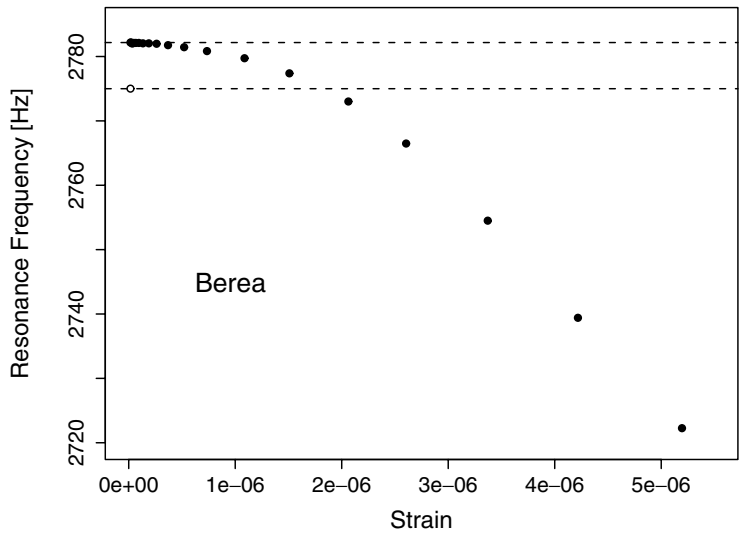

Fig. 26.1. Conditioning effect. The resonance frequency is plotted as a function of strain for Berea. The peak of the resonance curve is measured at different strains from low strain 10^{-9}up to 10^{-6}, the drive is then dropped of to the lowest strain. This last value (open dots) for f_R is different from the first one (full dot) as a consequence of conditioning.

strains from low strain 10^{-9} up to high strain 10^{-6}, and the external force is then reduced back to the lowest strain. The last value (open dots in Figure 26.1) for f_R is different from the first one (full dot): the reason for this difference is the conditioning.

The experimental data cannot be analyzed easily due to the presence of this nonequilibrium dynamics. In order to prevent this contamination, an ad hoc experimental strategy, named "zig–zag," was developed (see TenCate et al. in this book). This method consists of the systematical increase of the drive level passing through the up/down frequency sweeps and then releasing it back to the lowest strain to check if the f_R has changed.

3. Experimental Evidence

3.1 Two Regions

The samples analyzed are two sandstones, Berea and Fontainebleau. During the experiment the bar is driven by a frequency f and the acceleration of the bar end is measured. In order to compare samples with different length L the acceleration $\ddot{u}$ is converted into strain ϵ, using the convention $\epsilon = \ddot{u}/(4\pi L f^2)$. Different resonance curves are built at constant drive amplitude sweeping the frequency up/down (see Figure 26.2). In this experiment the frequency stability of the samples is $\simeq 0.1$ Hz corresponding to a thermal stability of 10 mK.

For each resonance curve the peak and the resonance frequency f_R are determined using a statistical analysis that was developed by D. Higdon of the Los Alamos National Laboratory. This analysis is based on a nonparametric Gaussian process to model the strain as a function of frequency (Banerjee et al., 2004). Using a Markov Chain Monte Carlo (MCMC) method, a Bayesian estimation for the peak and f_R are calculated together with their uncertainties.

The application of the zig–zag method reveals the presence of two strain regions. These two regions are divided by a strain threshold ϵ_{th}, below which there is no evidence of conditioning (first region) and beyond which the measures are contaminated by nonequilibrium dynamics (second region). The threshold ϵ_{th} is a function of the material and environmental quantities such as temperature, saturation, and so on. The value of the threshold for Fontainebleau is $\epsilon_{th} = 2 \cdot 10^{-7}$ and $\epsilon_{th} = 5 \cdot 10^{-7}$ for

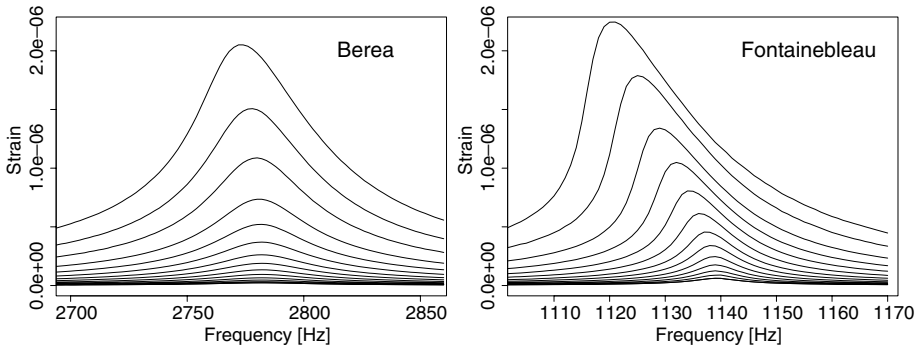

Fig. 26.2. Experimental resonance frequency curves for Berea and Fontainebleau.

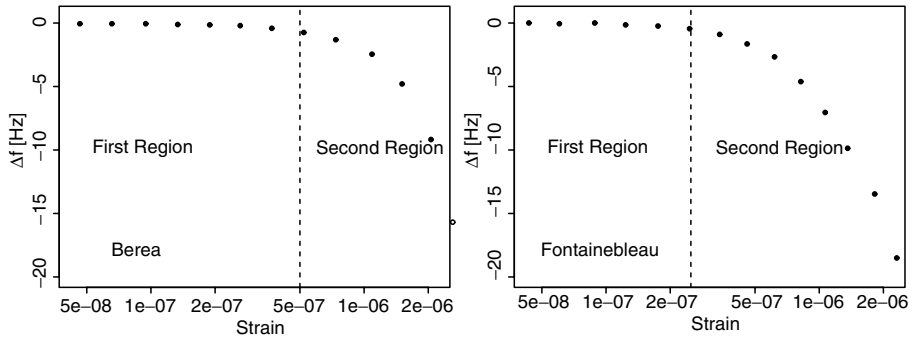

Fig. 26.3. Resonance frequency shift for both Berea and Fontainebleau. Dashed lines show the threshold.

Berea. In Figure 26.3, the shift of the resonance frequency for both samples is plotted as a function of strain. In the same figure the two regimes, nonconditioning and conditioning, are outlined.

In the first region, strain less than ϵ_{th}, there is no evidence of conditioning: Rocks show a reversible nonlinearity. The resonance frequency shift is repeatable: one can change how the experiment is carried out and the results do not change. In the absence of conditioning, the data show the intrinsic nonlinearity and consequently they can be simply analyzed and interpreted.

On the other hand, in the second region, strain bigger than ϵ_{th}, conditioning, and nonequilibrium dynamics are present. As a consequence, the experimental results are history dependent and not repeatable. Without a good understanding of the relationship between nonlinear dynamics and intrinsic nonlinearity, the data beyond that threshold cannot be simply interpreted to define intrinsic nonlinearity. Analysis of the data beyond ϵ_{th} without considering the nonequilibium contamination can only lead to erroneous conclusions.

3.2 First Region: Intrinsic Nonlinearity

Figure 26.4 shows the shift of the resonance frequency versus strain for the first region where the conditioning is not present. The strain range of this regime is $2 \cdot 10^{-9}$ to $2 \cdot 10^{-7}$ for Fontainebleau and $2 \cdot 10^{-9}$ to $5 \cdot 10^{-7}$ for Berea. The resonance frequency f_R and the respective strain are calculated using the MCMC method, which also computes the error bars. Note that the error bars for the strain are too small to be seen in Figure 26.4 for the strain range used.

The data analysis shows that f_R decreases quadratically as we increase the drive amplitude to the threshold ϵ_{th}. At very low strain, 10^{-8} to 10^{-7} , both rocks behave effectively as a linear elastic system: any change in the f_R can be seen in the error bars. There is no evidence of linear softening, which could lead one to believe in the presence of anomalous nonlinear behavior. In this region the data are well described by a classical nonlinear model, where the nonlinear term is represented by a Duffing nonlinearity (see the next section for model details). Figure 26.4 shows an excellent agreement between the experimental data and the fit using this theoretical model (solid lines). The quality factor Q is calculated as the ratio of the resonance frequency and

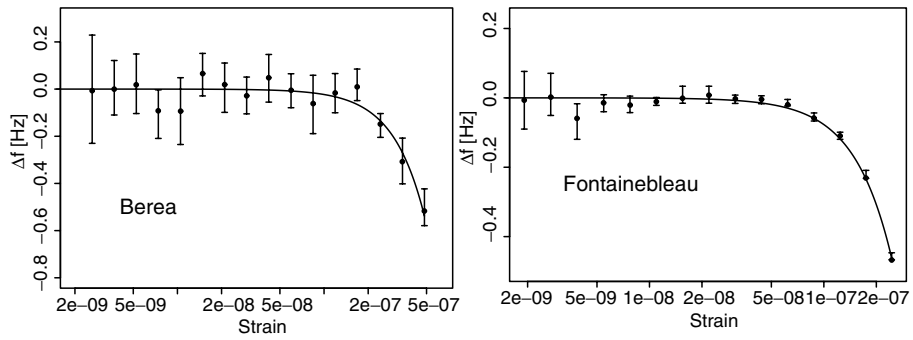

Fig. 26.4. First region: resonance frequency shift for Berea and Fontainebleau limited at the strain range where conditioning and memory effects do not occur. The solid lines are the theoretical fits: a classical Duffing nonlinear oscillator.

the width of the resonance curve at $1/\sqrt{2}$ of the maximum, Γ. It is important to point out that the uncertainties of the quality factor are larger than the ones of the resonance frequency peak. Analyzing the resonance curves, it is easy to see that Γ is constant within one percent. Therefore, the quality factor behaves as the resonance frequency, quadratically with the strain.

4. Model

As introduced in the previous section, in the low-strain regime the experimental data are accurately described by a simple phenomenological dynamical model. This model consists of a classical damped harmonic potential to which a quartic classical nonlinear term (Duffing) is added. The equation of motion for the displacement $u$can be written as follows.

$$\ddot{u} + \Omega_0^2 u + 2\mu\dot{u} + \gamma u^3 = F\sin(\omega t), \tag{26.1}$$

where Ω_0 is the linear resonance frequency, μ is the damping coefficient, and $\omega = 2\pi f$ is the angular frequency. $\gamma < 0$, the nonlinear parameter, leads to a softening nonlinearity as the experiments show. The amplitude of the driving force F is proportional to the amplitude of the voltage applied to the bar in the experiment. The derivation of an analytical approximation for the solution of Eq. (26.1) is given in detail in Nayfeh (1981) and leads to the following relation between the displacement amplitude, a, and the drive amplitude F.

$$\Omega_0^2\mu^2a^2 + a^2\left[(\omega - \Omega_0)\Omega_0 - \frac{3}{8}a^2\gamma\right]^2 = \frac{1}{4}F^2. \tag{26.2}$$

The peak of the resonance curve a_R, and the drive frequency $\omega_R = 2\pi f_R$, at which the peak occurs, can be easily calculated from Eq. (26.2):

$$\begin{cases} a_r &= \frac{F}{2\mu\Omega_0} \\ \omega_R &= \frac{3F^2\gamma}{32\mu^2\omega_0^3} + \Omega_0. \end{cases} \tag{26.3}$$

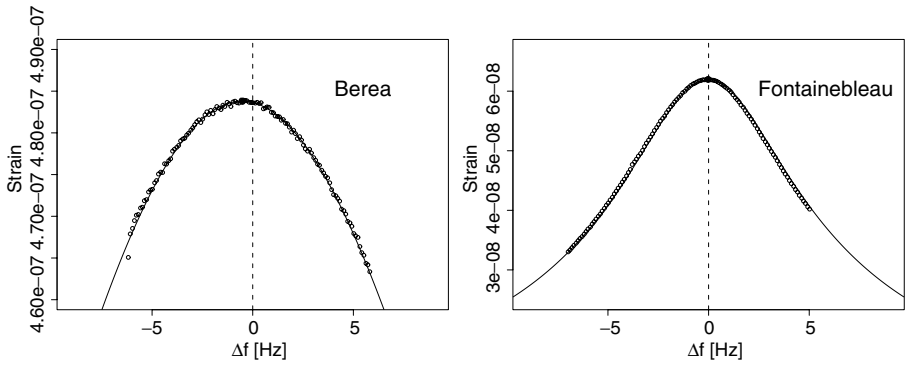

Fig. 26.5. First region: resonance frequency curve for Berea and Fontainebleau limited to the strain range where conditioning and memory effects do not occur. Solid lines are the theoretical model, open circles represent the experimental data, and full dots are the resonance frequency peaks calculated using MCMC.

The previous equation can be written in terms of the effective strain ϵ and the resonance frequency f_R as

$$f_R = \frac{3L^2\gamma}{16\pi^3\Omega_0}\epsilon^2 + \frac{\Omega_0}{2\pi}. \tag{26.4}$$

Thus, in agreement with the measured data, the model predicts that the resonance frequency softens quadratically with the amplitude F, which is proportional to the strain amplitude. In Figure 26.4 the experimental data are fitted using the second equation in (26.3). The fitting parameters, Ω_0 and γ, are determined for both samples: for the Fontainebleau sample $\Omega_0 = 7262.8\,\mathrm{rad/s}$, $\gamma = -7.6 \times 10^{19}\,\mathrm{m^{-2}\,s^{-2}}$, and for the Berea sample, $\Omega_0 = 17375.7\,\mathrm{rad/s}$, $\gamma = -5.3 \times 10^{19}\,\mathrm{m^{-2}\,s^{-2}}$. Once the parameters Ω_0 and γ are fixed as just described, the resonance curves are reconstructed and compared with the experimental resonance curves in Figure 26.5. Both Figures 26.4 and 26.5 show an excellent agreement between theoretical prediction and measured data. The model also predicts that the width of the resonance curve is independent of the drive amplitude. Its theoretical value $\Gamma = 2\mu$ is in agreement with the experimental evidence.

5. Conclusions

The main idea presented in this chapter is that we need to be careful interpreting the experimental data to provide a basis for the existence of nonclassical behavior. Two strain regions have been delineated by a strain threshold, ϵ_{th}, which is material and environment dependent. The one at low strain is free of conditioning and memory effects and as a consequence the experiment is repeatable. In the second region the external force drives the sample into a new nonequilibrium state. Then the resonance frequency shift is not reversible anymore. Meanwhile in the first region the rock shows its intrinsic nonlinearity and the measured data can be simply interpreted; in the second region the data contaminated by the nonequilibrium dynamics do not have a simple interpretation.

Limiting the analysis to the first region, it has been found that rocks do not show a nonclassical nonlinearity as it was claimed in previous works (Smith and TenCate, 2000, Guyer et al., 1999). A classical Duffing nonlinearity is enough to capture the dynamical behavior in this region. A detailed explanation about the disagreement with previous works can be found in Pasqualini (submitted). Anomalous features can be [AQ2] seen only in the region where the nonequilibrium dynamics contaminates the intrinsic nonlinearity and one cannot simply interpret this behavior as a sign of nonclassical nonlinearity in rocks.

As a consequence of this experimental evidence it is clear that we need a new theory that combines the intrinsic nonlinearity of the materials and nonequilibrium dynamics. We cannot speak about nonclassical nonlinearity in rocks until the fundamental relationship between intrinsic nonlinearity and nonequilibrium dynamics is understood.

Acknowledgments

The results presented in this chapter have been obtained in collaboration with several colleagues at Los Alamos National Laboratory. The theoretical part was done in collaboration with Salman Habib (T8) and Katrin Heitmann (ISR1), whereas the experimental part was done in collaboration with James A. TenCate (EES11). David Higdon (D1) developed the MCMC code.

This work was funded in part by the Institutional Support of Los Alamos through the Office of Basic Energy Science and Institute of Geophysics and Planetary Physics of Los Alamos National Laboratory (IGPP). I would like to thank Paolo Patelli for several discussions about the data analysis.

References

Banerjee, S., Carlin, B.P., and Gelfand, A.E., 2004, *Hierarchical Modeling and Analysis for Spatial Data*, Chapman and Hall/CRC Press, Boca Raton, FL.

Cook, N.G.W., Hodgson, K., 1965, Some detailed stressstrain curves for rock, *J. Geophys. Res.* **70**(12):2883–2888.

Gordon, R.B. and Davis, L.A., 1967, *J. Geophys. Res.* **73**:3917.

Guyer, R.A. and Johnson, P.A., 1999, Nonlinear mesoscopic elasticity, evidence for a new class of materials, *Phys. Today*, **52**:30–35.

Guyer, R.A., TenCate, J., and Johnson, P.A., 1999, Hysteresis and the dynamic elasticity of consolidated granular materials, *Phys. Rev. Lett.* **82**:3280–3283.

Johnson, P.A., this book.

Johnson, P.A., Zinszner, B., and Rasolofosaon, P.N.J., 1996, Resonance and elastic nonlinear phenomena in rock, *J. Geophys. Res.* **101**:11553–11564.

Landau, L.D., and Lifshitz, E.M., 1998, *Theory of Elasticity*, Butterworth-Heinemann, Boston.

Nayfeh, A.H., 1981, *Introduction to Perturbation Techniques*, Wiley, New York; Schmidt, G., and Tondl, A., 1986, *Non-Linear Vibrations*, Cambridge University Press, New York.

Pasqualini, D., Heitmann, K., TenCate, J.A., Habib S., Higdon, D., and Johnson, J.A., [AQ2] submitted to *J. Geophys. Res*.

Smith, D.E. and TenCate, J., 2000, Sensitive determination of the nonlinear properties of Berea sandstone at low strains, *Geophys. Res. Lett.* **27**:1985–1988.

TenCate, J.A., et al. this book.

TenCate, J.A., Pasqualini, D., Habib, S., Heitmann, K., Higdon, D., and Johnson, P.A., 2004, Nonlinear and Nonequilibrium Dynamics in Geomaterials, *Phys. Rev. Lett.* **93**:065501–1–065501–4.

TenCate, J.A., Shankland, T.J., 1996, Slow dynamics in the nonlinear elastic response of Berea sandstone, *Geophys. Res. Lett.* **23**:3019–3022.

TenCate, J.A., Smith, E., Guyer, R. A., 2000, Universal slow dynamics in granular solids, *Phys. Rev. Lett.* **85**(5):1020–1023.

Author Queries:-

AQ1: Please update.

AQ2: Please update.